

## Longitudinal structure function from logarithmic slopes of $F_2$ at low $x$

G. R. Boroun\*

*Physics Department, Razi University, Kermanshah 67149, Iran*

 (Received 15 July 2017; revised manuscript received 18 November 2017; published 22 January 2018)

Using Laplace transform techniques, I calculate the longitudinal structure function  $F_L(x, Q^2)$  from the scaling violations of the proton structure function  $F_2(x, Q^2)$  and make a critical study of this relationship between the structure functions at leading order (LO) up to next-to-next-to leading order (NNLO) analysis at small  $x$ . Furthermore, I consider heavy quark contributions to the relation between the structure functions, which leads to compact formula for  $N_f = 3 + \text{Heavy}$ . The nonlinear corrections to the longitudinal structure function at LO up to NNLO analysis are shown in the  $N_f = 4$  (light quark flavor) based on the nonlinear corrections at  $R = 2$  and  $R = 4 \text{ GeV}^{-1}$ . The results are compared with experimental data of the longitudinal proton structure function  $F_L$  in the range of  $6.5 \leq Q^2 \leq 800 \text{ GeV}^2$ .

DOI: [10.1103/PhysRevC.97.015206](https://doi.org/10.1103/PhysRevC.97.015206)

### I. INTRODUCTION

The inclusive deep inelastic scattering (DIS) measurements are of importance to understanding the gluonic substructure of proton at low values of the Bjorken variable  $x$ . The reduced cross section is defined in the following form:

$$\tilde{\sigma}(x, Q^2) = F_2(x, Q^2) - \frac{y^2}{Y_+} F_L(x, Q^2), \quad (1)$$

where  $Y_+ = 1 + (1 - y)^2$ ,  $y = Q^2/xs$  is the inelasticity,  $s$  is the center-of-mass squared energy of incoming electrons and protons, and  $F_2(x, Q^2)$  and  $F_L(x, Q^2)$  are the transverse and longitudinal structure functions, respectively.

The structure functions describe the momentum distributions of partons in a nucleon. A measurement of the proton structure functions ( $F_2$  and  $F_L$ ) at low  $x$  is directly sensitive to the gluon density. This provides a sensitive test for perturbative QCD (pQCD).

The longitudinal structure function is determined by measurements of differential cross sections at different values of  $\sqrt{s}$  at the Hadron-Electron Ring Accelerator (HERA) at DESY, where data on  $\sqrt{s}$  for electron beam energies of  $E_e \simeq 27.5 \text{ GeV}$  and for proton beam energies of  $E_p = 920, 820, 575, \text{ and } 460 \text{ GeV}$  are collected [1,2]. The experimental data for neutral current were also collected for  $0.045 \leq Q^2 \leq 50\,000 \text{ GeV}^2$  and  $6E - 7 \leq x \leq 0.65$  at values of the inelasticity  $0.005 \leq y \leq 0.95$ .

The contribution of  $F_L$  to reduced cross section [Eq. (1)] is significant only at high value of the inelasticity  $y$ , i.e.,

the kinematic region. The latter case corresponds to the low values of the Bjorken variable  $x$ , and the longitudinal structure function is related to the gluon density of the proton. Because gluons exert the most influence at low  $x$ , the quark contribution to the longitudinal structure function and singlet structure function is ignored in next step.

The gluonic longitudinal structure function can be written as

$$x^{-1} F_L(x, Q^2) = \langle e^2 \rangle C_{L,g}(\alpha_s, x) \otimes g(x, Q^2), \quad (2)$$

where  $g(x, Q^2)$  represents the gluon density, and  $\langle e^2 \rangle$  is the average squared charge ( $=5/18$  for even  $N_f$ , where  $N_f$  denotes number of active light flavors). The symbol  $\otimes$  denotes the Mellin convolution according to the usual prescription.

The perturbative expansion of the gluon coefficient function can be written as

$$C_{L,g}(\alpha_s, x) = \sum_{n=1} \left( \frac{\alpha_s}{4\pi} \right)^n c_{L,g}^n(x), \quad (3)$$

where  $n$  is the order in the running coupling constant.

The reduced cross section for deep inelastic lepton-nucleon scattering [Eq. (1)] is defined in terms of the proton structure function  $F_2$ . At low values of  $x$ , the gluon contribution to the proton structure function  $F_2$  dominates over the flavor singlet contribution. The Dokshitzer–Gribov–Lipatov–Altarelli–Parisi (DGLAP) evolution equation for gluon dominating  $F_2$  structure function is given by

$$\frac{\partial F_2^s(x, Q^2)}{\partial \ln(Q^2)} = \frac{\alpha_s(Q^2)}{2\pi} P_{qg}(\alpha_s, x) \otimes G(x, Q^2), \quad (4)$$

where  $F_2^s$  is the singlet distribution function. The splitting function  $P_{qg}$  is the leading order (LO) up to high-loop corrections to the QCD  $\beta$  function as

$$P_{qg}(\alpha_s, x) = P_{qg}^{\text{LO}} + \frac{\alpha_s(Q^2)}{2\pi} P_{qg}^{\text{NLO}} + \dots \quad (5)$$

Several methods to relate  $F_L$  and  $F_2$  scaling violation to the gluon density at small  $x$  were suggested previously [3,4]. These

\*grboroun@gmail.com; boroun@razi.ac.ir

Published by the American Physical Society under the terms of the [Creative Commons Attribution 4.0 International](https://creativecommons.org/licenses/by/4.0/) license. Further distribution of this work must maintain attribution to the author(s) and the published article's title, journal citation, and DOI. Funded by SCOAP<sup>3</sup>.

methods were proposed to isolate the gluon distribution by its expansion around  $z = \frac{1}{2}$ . In LO analysis with  $N_f = 4$ , the authors of Ref. [3] suggested an approximate relation between the gluon density at the point  $2.5x$  and the longitudinal structure function  $F_L$  at the point  $x$  in the following form:

$$F_L(x, Q^2) = \frac{2\alpha_s}{\pi} \frac{\sum_{i=1}^{N_f} e_i^2}{5.9} G(2.5x, Q^2). \quad (6)$$

Equation (6) was derived in an expansion of gluon distribution around  $z = \frac{1}{2}$ . A similar relation for the derivation of  $F_2(x, Q^2)$  with respect to  $\ln Q^2$  based on the expansion of the gluon distribution around  $z = \frac{1}{2}$  was found in Ref. [4], where the following result was obtained:

$$\frac{\partial F_2(x, Q^2)}{\partial \ln Q^2} = \frac{5\alpha_s}{9\pi} \frac{2}{3} G(2x, Q^2). \quad (7)$$

Combining Eqs. (6) and (7), one could calculate the longitudinal structure function by derivation of the structure function at a rescaled value  $\frac{\zeta_2}{\zeta_L} x$ , where  $\zeta_2 \simeq 0.5$  and  $\zeta_L \simeq 0.4$ . The corresponding LO expression is

$$F_L(x, Q^2) = \frac{\partial F_2(\eta x, Q^2)}{\partial \ln Q^2}, \quad (8)$$

where  $\eta \simeq 1.25$ .

In addition, two different methods were suggested [5,6], the derivatives of the structure functions were based in the expansion of the gluon distribution around the arbitrary point  $z = \alpha$ . The results were derived at an arbitrary point of expansion as follows:

$$F_L(x, Q^2) = \frac{10\alpha_s}{27\pi} G\left(\frac{x}{1-\alpha} \left(\frac{3}{2} - \alpha\right), Q^2\right), \quad (9)$$

and

$$\frac{\partial F_2(x, Q^2)}{\partial \ln Q^2} = \frac{10\alpha_s}{27\pi} G\left(\frac{x}{1-\alpha} \left(\frac{3}{2} - \alpha\right), Q^2\right). \quad (10)$$

Equations (9) and (10) strongly depend on the momentum fraction carried by gluons in Eqs. (2) and (4) and show the behavior of the gluonic structure functions based on the expansion of the gluon distribution around  $z = \alpha$ .

In this paper I introduce a method to calculate structure functions by using the Laplace transform techniques. The paper is organized as follows: In Sec. II, I find the relation between the structure functions at small  $x$  at LO analysis. In Sec. III, I consider the high-order corrections to the relation between the structure functions. In Sec. IV, I utilize the solution obtained to calculate the nonlinear behavior of the longitudinal structure function at the hot-spot point in the LO analysis and present an analytical analysis of the longitudinal structure function. Then I compare the result obtained with H1 experimental data. In Sec. V, I study the high-order corrections to the nonlinear behavior of the longitudinal structure function. My conclusion is given in Sec. VI. In Appendix A, I present the results for the splitting functions and coefficients in the inverse Laplace transform method at some values of  $Q^2$ . Appendix B includes the analytical expression for  $F_2^{pp}(x, Q^2)$ . In Appendixes C and D, I present the high-order corrections and high-order ratios at NLO up to NNLO at small  $x$ . Appendix E deals with a

technical detail including the inverse Laplace transform of the nonlinear kernels at LO and high-order corrections presented in Appendix F.

## II. GENERAL METHOD

In pQCD, the evolution equations for proton and longitudinal structure functions are given in terms of the nonsinglet, singlet, and gluon coefficient functions. At small values of  $x$  the gluon contribution to the structure functions dominate over the flavor singlet and nonsinglet contribution. Therefore, in this research I consider the gluonic structure functions evolution equations.

### A. Four flavours

One could write the LO equation for the evolution of the proton structure function at low values of  $x$  as

$$\frac{\partial F_2(x, Q^2)}{\partial \ln(Q^2)} = \frac{10}{18} \frac{\alpha_s(Q^2)}{\pi} \int_x^1 \frac{x}{y^2} P_{qg}^{\text{LO}}\left(\frac{x}{y}\right) G(y, Q^2) dy. \quad (11)$$

The longitudinal structure function for gluon dominating is given by

$$F_L(x, Q^2) = \frac{20}{9} \frac{\alpha_s(Q^2)}{\pi} \int_x^1 \frac{1}{y} c_{L,g}^{\text{LO}}\left(\frac{x}{y}\right) G(y, Q^2) dy. \quad (12)$$

Considering the coordinate transformation as  $v = \ln(1/x)$  and  $\omega = \ln(1/y)$  [7], one could rewrite Eqs. (11) and (12) with respect to these variables:

$$\widehat{\mathcal{F}}_2(v, Q^2) = \int_0^v \widehat{G}(\omega) e^{-(v-\omega)} (1 - 2e^{-(v-\omega)} + 2e^{-2(v-\omega)}) d\omega, \quad (13)$$

and

$$\widehat{\mathcal{F}}_L(v, Q^2) = \int_0^v \widehat{G}(\omega) e^{-2(v-\omega)} (1 - e^{-(v-\omega)}) d\omega, \quad (14)$$

where

$$\begin{aligned} \widehat{f}(v, Q^2) &= f(e^{-v}, Q^2), \\ \widehat{\mathcal{F}}_2(v, Q^2) &= \frac{18\pi}{10\alpha_s} \frac{\partial \widehat{F}_2(v, Q^2)}{\partial \ln(Q^2)}, \\ \widehat{\mathcal{F}}_L(v, Q^2) &= \frac{9\pi}{20\alpha_s} \widehat{F}_L(v, Q^2). \end{aligned}$$

Defining the Laplace transforms  $\widehat{\mathcal{F}}_2(s, Q^2) = \mathcal{L}[\widehat{F}_2(v, Q^2); s]$  and  $\widehat{\mathcal{F}}_L(s, Q^2) = \mathcal{L}[\widehat{\mathcal{F}}_L(v, Q^2); s]$  explicitly from Eqs. (13) and (14), one obtains the structure functions in  $s$  space as

$$\mathcal{F}_2(s, Q^2) = g(s, Q^2) \Theta_2(s), \quad (15)$$

and

$$\mathcal{F}_L(s, Q^2) = g(s, Q^2) \Theta_L(s). \quad (16)$$

In Eqs. (15) and (16) I used the fact that the Laplace transform of a convolution function is simply ordinary product of the Laplace transform of that function. Taking into account the

gluon distribution, one could extend the Laplace transformation to the high-order corrections in the following form:

$$\mathcal{F}_2(s, Q^2) = g(s, Q^2) \left[ \Theta_2^{\text{LO}}(s) + \frac{\alpha_s}{4\pi} \Theta_2^{\text{NLO}}(s) + \dots \right], \quad (17)$$

and

$$\mathcal{F}_L(s, Q^2) = g(s, Q^2) \left[ \Theta_L^{\text{LO}}(s) + \frac{\alpha_s}{4\pi} \Theta_L^{\text{NLO}}(s) + \dots \right]. \quad (18)$$

The leading-order splitting functions in Laplace  $s$  space are given by

$$\Theta_2^{\text{LO}}(s) = \frac{1}{1+s} - \frac{2}{2+s} + \frac{2}{3+s}, \quad (19)$$

and

$$\Theta_L^{\text{LO}}(s) = \frac{1}{2+s} - \frac{1}{3+s}. \quad (20)$$

I obtain, therefore, the derivative of the structure function in the form of the longitudinal structure function in  $s$  space as

$$\frac{\partial F_2(s, Q^2)}{\partial \ln(Q^2)} = \frac{1}{4} h(s) F_L(s, Q^2), \quad (21)$$

or

$$F_L(s, Q^2) = 4h^{-1}(s) \frac{\partial F_2(s, Q^2)}{\partial \ln(Q^2)}, \quad (22)$$

where  $h(s) = \frac{\Theta_2^{\text{LO}}(s)}{\Theta_L^{\text{LO}}(s)}$ .

The inverse Laplace transforms of  $h(s)$  and  $h^{-1}(s)$  is given by the kernels  $\widehat{\eta}(v) \equiv \mathcal{L}^{-1}[h(s); v]$  and  $\widehat{J}(v) \equiv \mathcal{L}^{-1}[h^{-1}(s); v]$ . Therefore, I have

$$\widehat{\eta}(v) = 2\delta(v) + \delta'(v) + 2e^{-v}, \quad (23)$$

and

$$\widehat{J}(v) = e^{-\frac{3}{2}v} \cos\left(\frac{1}{2}\sqrt{7}v\right) - \frac{1}{7}\sqrt{7}e^{-\frac{3}{2}v} \sin\left(\frac{1}{2}\sqrt{7}v\right). \quad (24)$$

Consequently, the general relation between the structure functions in  $x$  space is given by

$$\begin{aligned} \frac{\partial F_2(x, Q^2)}{\partial \ln(Q^2)} &= \frac{1}{2} F_L(x, Q^2) - \frac{1}{4} x \frac{\partial F_L(x, Q^2)}{\partial x} \\ &+ \frac{1}{2} \int_x^1 F_L(y, Q^2) \frac{x}{y^2} dy. \end{aligned} \quad (25)$$

Finally, one could write the leading-order relation for the longitudinal structure function for massless quarks in the form of the derivative of the structure function as

$$\begin{aligned} F_L(x, Q^2)|_{N_f=4} &= 4 \int_x^1 \frac{\partial F_2(y, Q^2)}{\partial \ln(Q^2)} \left(\frac{x}{y}\right)^{3/2} \left[ \cos\left(\frac{\sqrt{7}}{2} \ln \frac{y}{x}\right) \right. \\ &\left. - \frac{\sqrt{7}}{7} \sin\left(\frac{\sqrt{7}}{2} \ln \frac{y}{x}\right) \right] \frac{dy}{y}. \end{aligned} \quad (26)$$

### B. Three flavors + heavy

The heavy quark contribution (charm and bottom) to the relation between  $F_L$  and  $F_2$  is define by a fixed-order number scheme using  $m_c = 1.5$  GeV and  $m_b = 4.5$  GeV [8]. The mass

of these heavy quarks satisfies  $m_Q \gg \Lambda_{\text{QCD}}$ , and provides a hard scale for pQCD calculations. One could consider the perturbative predictions for the longitudinal structure function.

Equation (2) can be rewritten in the convolution form:

$$\begin{aligned} x^{-1} F_L(x, Q^2) &= \langle e^2 \rangle|_{N_f=3} C_{L,g}(\alpha_s, x) \otimes g(x, Q^2) \\ &+ x^{-1} F_L^c + x^{-1} F_L^b, \end{aligned} \quad (27)$$

where  $\otimes$  in the  $N_f = 3$  for massless quarks u, d, and s denotes the common convolution, and  $F_L^{c(b)}$  are heavy quark corrections to the longitudinal structure function at small  $x$ .

These corrections in deep inelastic electron-proton-scattering collisions serve as a test of pQCD and the heavy quark production is directly sensitive to the gluon density and heavy-quark mass. One should write the individual longitudinal structure functions as

$$F_L(x, Q^2) = F_L^g + F_L^{\text{heavy}}. \quad (28)$$

At small  $x$ , where the gluon distribution is dominant, the heavy-quark contributions  $F_k^i(x, Q^2, m_i^2)$  with  $i = b, c$  and  $k = 2, L$  in the proton structure function is written as

$$\begin{aligned} F_k^i(x, Q^2, m_i^2) &= C_{g,k}^i(x, Q^2) \otimes g(x, Q^2) \\ &= 2x e_i^2 \frac{\alpha_s(\mu^2)}{2\pi} \int_{ax}^1 \frac{dy}{y} C_{g,k}^i\left(\frac{x}{y}, Q^2\right) g(y, \mu^2), \end{aligned} \quad (29)$$

where  $a = 1 + 4\frac{m_i^2}{Q^2}$ , and the renormalization scale  $\mu$  is assumed to be the average  $\langle \mu^2 \rangle = 4m_i^2 + \frac{Q^2}{2}$ .

Using the Laplace transform method [7], one can rewrite the heavy structure functions in terms of the convolution integrals with respect to  $v'$  and  $\omega'$  variables at small  $x$  as

$$\begin{aligned} F_k^i\left(\frac{1}{a}v', Q^2\right) &= \int_0^{v'} \widehat{G}(\omega', Q^2) \frac{1}{a} e^{-(v'-\omega')} C_{g,k}^i\left(\frac{1}{a}e^{-(v'-\omega')}\right) d\omega', \end{aligned} \quad (30)$$

where

$$\widehat{H}_k^i(v') \equiv \frac{1}{a} e^{-v'} C_{g,k}^i\left(\frac{1}{a}e^{-v'}\right). \quad (31)$$

Here  $v' = \ln \frac{1}{ax}$ ,  $\omega' = \ln \frac{1}{a\omega}$ , and

$$F_k^i\left(\frac{1}{a}v', Q^2\right) \equiv \left(2\frac{\alpha_s^{\text{LO}}(\mu^2)}{2\pi} e_i^2\right)^{-1} \widehat{F}_k^i. \quad (32)$$

The Laplace transformation of  $\widehat{H}_k^i(v')$  is given by  $h_k^i(s)$ , where

$$h_k^i(s) \equiv \mathcal{L}[\widehat{H}_k^i(v'); s] = \int_0^\infty \widehat{H}_k^i(v') e^{-sv'} dv'. \quad (33)$$

The convolution theorem for Laplace transforms allows one to rewrite the heavy distribution functions as a product of their

Laplace transforms  $g(s, Q^2)$  and  $h_k^i(s)$ . In this case one has

$$\begin{aligned} FF_2^i(s, Q^2) &= \mathcal{L} \left[ \int_0^{v'} \hat{G}(\omega', Q^2) \hat{H}_2^i(v' - \omega'); s \right] \\ &= g(s, Q^2) h_2^i(s), \end{aligned} \quad (34)$$

and

$$\begin{aligned} FF_L^i(s, Q^2) &= \mathcal{L} \left[ \int_0^{v'} \hat{G}(\omega', Q^2) \hat{H}_L^i(v' - \omega'); s \right] \\ &= g(s, Q^2) h_L^i(s). \end{aligned} \quad (35)$$

Therefore the ratio of the heavy structure functions are independent of the gluon distribution function in  $s$  space. This ratio can be written as

$$\frac{F_L^i(s)}{F_2^i(s)} = \frac{h_L^i(s)}{h_2^i(s)}. \quad (36)$$

If one takes the inverse Laplace transformation of Eq. (36), then one has

$$F_L^i(v') = \mathcal{L}^{-1} [F_2^i(s) R h^i(s); v'], \quad (37)$$

where  $R h^i(s) = \frac{h_L^i(s)}{h_2^i(s)}$ .

Here I used the following property for inverse Laplace transformation:

$$\begin{aligned} \mathcal{L}^{-1} [F(s)G(s)] &= \int_0^t f(t - \tau)g(\tau)d\tau \\ &= \int_0^t g(t - \tau)f(\tau)d\tau. \end{aligned} \quad (38)$$

Then Eq. (37) becomes as

$$F_L^i(v', Q^2) = \int_0^{v'} F_2^i(\omega', Q^2) \hat{J}^i(v' - \omega') d\omega', \quad (39)$$

where  $\hat{J}^i(v') = \mathcal{L}^{-1} [R h^i(s); v']$ .

The analytical results for the parameters  $\hat{J}^i$  for a particular range of  $Q^2$  under study are given in Appendix A.

In a similar manner, the longitudinal structure function can be determined at small  $x$  by considering the heavy corrections to the structure function. Thus, applying the convolution theorem, the analytical solution for the longitudinal structure function for  $N_f = 3 + \text{Heavy}$  should be converted to the usual  $(x, Q^2)$  space. Therefore, one has

$$\begin{aligned} F_L(x, Q^2)|_{N_f=3+\text{Heavy}} &= \frac{16}{5} \int_x^1 \frac{\partial F_2(y, Q^2)}{\partial \ln(Q^2)} \left(\frac{x}{y}\right)^{3/2} \left[ \cos\left(\frac{\sqrt{7}}{2} \ln \frac{y}{x}\right) \right. \\ &\quad \left. - \frac{\sqrt{7}}{7} \sin\left(\frac{\sqrt{7}}{2} \ln \frac{y}{x}\right) \right] \frac{dy}{y} + \int_{ax}^1 \frac{dy}{y} F_2^c(y, Q^2) J^c\left(\frac{x}{y}, Q^2\right) \\ &\quad + \int_{ax}^1 \frac{dy}{y} F_2^b(y, Q^2) J^b\left(\frac{x}{y}, Q^2\right). \end{aligned} \quad (40)$$

One observes that the connection between the structure functions [in Eqs. (26) and (40)] are independent of the running coupling constant at LO analysis and gluon density behavior. To calculate the right-hand side of these equations [Eqs. (26)

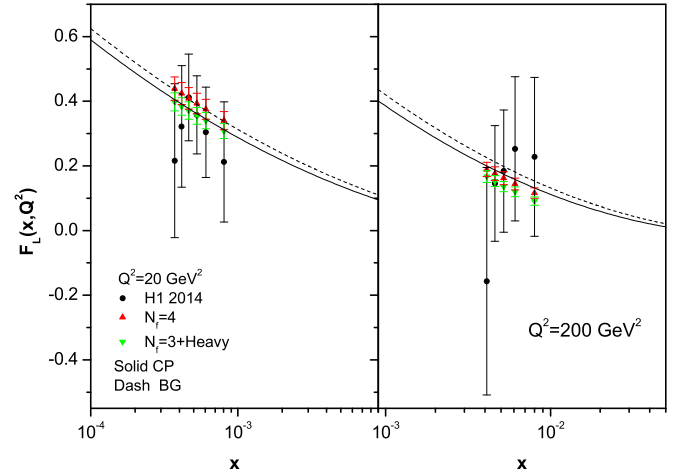


FIG. 1. The longitudinal structure functions  $F_L(x, Q^2)$  [up triangle ( $N_f = 4$ ), down triangle ( $N_f = 3 + \text{Heavy}$ )] compared by H1 [1] (circles) at the given values of  $Q^2$  accompanied by total uncertainties. The determined error bars represent the derivative of  $F_2(x, Q^2)$  uncertainties. The curves represent the prediction from the expanding of gluon behavior [3–6].

and (40)], one has to have an expression for the proton structure function [9] and heavy quark structure [10] functions for massless and heavy quarks.

The H1 Collaboration reported a measurement of inclusive  $ep$  cross sections at high  $Q^2$  at  $\sqrt{s} = 225$  and  $252$  GeV. HERA provided the first measurements of  $F_L$  in the region  $120 \leq Q^2 \leq 800$  GeV<sup>2</sup> and  $6.5 \times 10^{-4} < x < 0.032$  [1]. My results are compared with extracted longitudinal proton structure function  $F_L$  in the range of  $6.5 \leq Q^2 \leq 800$  GeV<sup>2</sup>.

In Fig. 1 the determined longitudinal structure function  $F_L$  is shown for  $Q^2 = 20$  GeV<sup>2</sup> and  $200$  GeV<sup>2</sup>. In this figure, the longitudinal structure functions determined for four massless quarks at  $m_c^2 < \mu^2$  and also to account for fixed the  $N_f = 3$  flavor number scheme as the heavy-flavor contributions to  $F_L$  are taken as given by fixed order perturbation theory. The results for  $Q^2 = 20$  and  $200$  GeV<sup>2</sup> are presented for  $N_f = 4$  and  $N_f = 3 + \text{Heavy}$  and are compared with H1 Collaboration data [1]. For heavy contributions to  $F_L$ , the renormalization scale is  $\langle \mu^2 \rangle = 4m_H^2 + Q^2/2$ . These results are accompanied

TABLE I. Parameters of Eq. (65), resulting from a global fit to the HERA combined data.

Parameter	Value
$a_0$	$-8.471 \times 10^{-2} \pm 2.62 \times 10^{-3}$
$a_1$	$4.190 \times 10^{-2} \pm 1.56 \times 10^{-3}$
$a_2$	$-3.976 \times 10^{-3} \pm 2.13 \times 10^{-4}$
$b_0$	$1.292 \times 10^{-2} \pm 3.62 \times 10^{-4}$
$b_1$	$2.473 \times 10^{-4} \pm 2.46 \times 10^{-4}$
$b_2$	$1.642 \times 10^{-3} \pm 5.52 \times 10^{-5}$
$F_p$	$0.413 \pm 0.003$
$\chi^2(\text{goodnessoffit})$	1.17

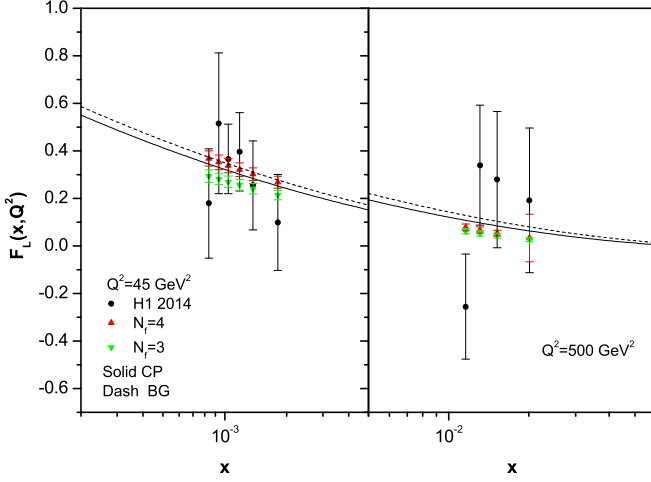


FIG. 2. The same as Fig. 1 at the given values of  $Q^2$  for  $N_f = 4$  and  $N_f = 3$ .

with errors due to fit parametrizations of  $\partial F_2/\partial \ln Q^2$ , as listed in Appendix B and Table I. It is seen from Fig. 1 that the results are comparable with the experimental data as accompanied with total errors, although those are independent of the gluon behavior. I also present the Cooper–Prytz (CP) fit [3,4], which depends on expanding the gluon distribution at  $z = 1/2$ , and the Gay Ducati–Boroun (BG) fit [5,6] which depends on expanding of the gluon distribution at  $z = \alpha$ .

In Fig. 2 I present the longitudinal structure function  $F_L$  for  $Q^2 = 45$  and  $500 \text{ GeV}^2$  without considering the heavy-quark contributions in the same Fig. 1. The longitudinal proton structure function  $F_L(x, Q^2)$  compared by averaging  $F_L$  data from Table 5 in Ref. [1] at the given values of  $Q^2$  and  $x$  with total uncertainty on  $F_L$ , shown in Fig. 3. A reasonable agreement between the longitudinal structure function as extracted from the direct measurement of the derivative of  $F_2$  with the experimental data is observed at moderate and high  $Q^2$  values at low values of  $x$ .

These results extend from the LO up to NNLO analysis with respect to the Laplace transform method at small  $x$  and I will try to compare our result with experimental data in the next section.

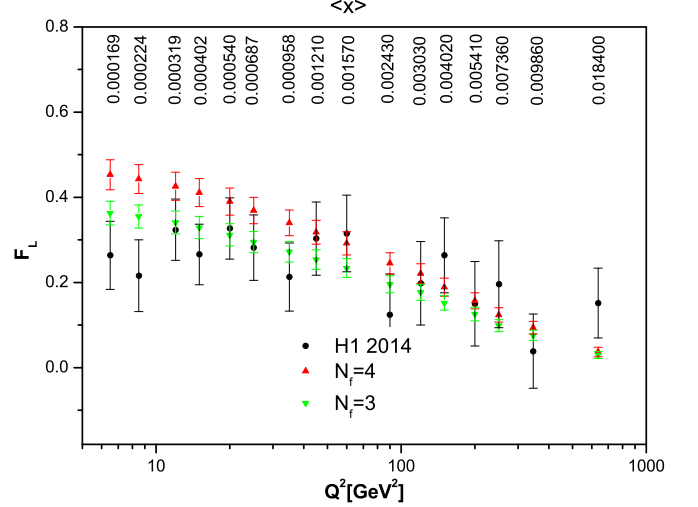


FIG. 3. The longitudinal structure function  $F_L$  compared with H1 data averaged over  $x$  in the region  $6.5 \leq Q^2 \leq 800 \text{ GeV}^2$  (solid points). The error bars represent the full errors as obtained by the Monte Carlo procedure described in the Ref. [1]. For each  $Q^2$  the average value of  $x$  is given above each data point.

### III. HIGH-ORDER CORRECTIONS

An analytical solution based on the Laplace transformation for the relation between the longitudinal structure function in terms of a convolution of the derivative of  $F_2$  is obtained at LO accuracy in perturbative QCD in Sec. II. Some analytical solutions of the DGLAP evolution equation in next-to-leading order (NLO) analysis using the Laplace transform method have been presented in Ref. [11]. In Refs. [12,13], the authors have been reported the complete two- and three-order coefficient functions for the longitudinal structure functions in deep inelastic scattering (DIS). Now, a detailed analysis has been performed to find an analytical solutions of the longitudinal structure function into the derivative of the proton structure function with respect to  $\ln Q^2$ , using the repeated Laplace transform, at NLO up to NNLO approximation.

In  $s$  space, one can rewrite the gluonic structure functions equations in terms of the convolution integrals up to NNLO analysis. The Laplace transform of these equations converted to an ordinary first-order differential equations in  $s$  space as one has

$$\begin{aligned} \frac{\partial \ln F_2(s, Q^2)}{\partial \ln Q^2} &= \frac{5}{18} \frac{\alpha_s(Q^2)}{4\pi} \int_0^v \left[ \hat{P}^{\text{LO}}(v-\omega) + \frac{\alpha_s(Q^2)}{4\pi} \hat{P}^{\text{NLO}}(v-\omega) + \left( \frac{\alpha_s(Q^2)}{4\pi} \right)^2 \hat{P}^{\text{NNLO}}(v-\omega) \right] \hat{G}(\omega, Q^2) d\omega \\ &= \frac{5}{18} \frac{\alpha_s(Q^2)}{4\pi} \left[ \Theta_2^{\text{LO}}(s) + \frac{\alpha_s(Q^2)}{4\pi} \Theta_2^{\text{NLO}}(s) + \left( \frac{\alpha_s(Q^2)}{4\pi} \right)^2 \Theta_2^{\text{NNLO}}(s) \right] g(s, Q^2), \end{aligned} \quad (41)$$

and

$$\begin{aligned} F_L(s, Q^2) &= \langle e^2 \rangle \frac{\alpha_s(Q^2)}{4\pi} \int_0^v \left[ \hat{c}^{\text{LO}}(v-\omega) + \frac{\alpha_s(Q^2)}{4\pi} \hat{c}^{\text{NLO}}(v-\omega) + \left( \frac{\alpha_s(Q^2)}{4\pi} \right)^2 \hat{c}^{\text{NNLO}}(v-\omega) \right] \hat{G}(\omega, Q^2) d\omega \\ &= \langle e^2 \rangle \frac{\alpha_s(Q^2)}{4\pi} \left[ \Theta_L^{\text{LO}}(s) + \frac{\alpha_s(Q^2)}{4\pi} \Theta_L^{\text{NLO}}(s) + \left( \frac{\alpha_s(Q^2)}{4\pi} \right)^2 \Theta_L^{\text{NNLO}}(s) \right] g(s, Q^2), \end{aligned} \quad (42)$$

where the running coupling constants have the following forms in NLO and NNLO analysis, respectively:

$$\frac{\alpha_s^{\text{NLO}}}{4\pi} = \frac{1}{\beta_0 t} \left[ 1 - \frac{\beta_1 \ln t}{\beta_0^2 t} \right], \quad (43)$$

and

$$\frac{\alpha_s^{\text{NNLO}}}{4\pi} = \frac{1}{\beta_0 t} \left\{ 1 - \frac{\beta_1 \ln t}{\beta_0^2 t} + \frac{1}{(\beta_0 t)^2} \times \left[ \left( \frac{\beta_1}{\beta_0} \right)^2 (\ln^2 t - \ln t + 1) + \frac{\beta_2}{\beta_0} \right] \right\}, \quad (44)$$

where  $\beta_0 = \frac{1}{3}(33 - 2n_f)$ ,  $\beta_1 = 102 - \frac{38}{3}n_f$ , and  $\beta_2 = \frac{2857}{6} - \frac{6673}{18}n_f + \frac{325}{54}n_f^2$  are the one-loop, two-loop, and three-loop corrections to the QCD  $\beta$  function and  $\Lambda$  is the QCD cutoff parameter. The  $\Lambda_{\text{QCD}}$  parameter usually defined in NLO

and NNLO analyses as  $\Lambda_{\text{QCD}}^{(N_f=4)} = 347$  MeV and  $\Lambda_{\text{QCD}}^{(N_f=5)} = 251$  MeV [12,13], respectively.

The N<sup>n</sup>LO expansion coefficients are defined in Ref. [13] in Mellin space and one should present these splitting functions and coefficient functions in Appendix C. In detail the shape of the structure functions are dominated by the gluon density at low values of  $x$ . Therefore, one would find

$$F_L(x, Q^2) = \mathcal{L}^{-1}[H(s, Q^2)DF_2(s, Q^2); v], \quad (45)$$

where  $DF_2 \equiv \frac{\partial F_2}{\partial \ln Q^2}$ . The high-order  $H(v, Q^2)$  for four  $Q^2$  values is presented in Appendix D. One can easily determine these high-order corrections to the gluonic longitudinal structure function based on the derivative of the proton structure function with respect to  $\ln Q^2$  at low  $x$ . Now considering the terms from NLO up to NNLO, the gluonic longitudinal structure function takes the following form for a given  $Q^2$  value:

$$\begin{aligned} F_L^{\text{NLO}}(x, Q^2)|_{Q^2=20 \text{ GeV}^2} &= -0.07DF_2(x, Q^2) + \int_x^1 \frac{dy}{y} DF_2(y, Q^2) \left[ -0.13 \left( \frac{x}{y} \right)^{0.08} + \left( \frac{x}{y} \right)^{1.54} \left[ 3.73 \cos \left[ 1.33 \ln \left( \frac{x}{y} \right) \right] \right. \right. \\ &\quad \left. \left. - 1.68 \left\{ \sin \left[ 1.33 \ln \left( \frac{x}{y} \right) \right] \right\} \right] \right], \\ F_L^{\text{NNLO}}(x, Q^2)|_{Q^2=20 \text{ GeV}^2} &= -0.31DF_2(x, Q^2) + \int_x^1 \frac{dy}{y} DF_2(y, Q^2) \left[ \left( \frac{y}{x} \right)^{0.06} \left\{ -0.3 \cos \left[ 0.26 \ln \left( \frac{x}{y} \right) \right] + 0.11 \right. \right. \\ &\quad \left. \left. \times \sin \left[ 0.26 \ln \left( \frac{x}{y} \right) \right] \right\} + \left( \frac{x}{y} \right)^{1.40} \left( 3.82 \cos \left[ 1.31 \ln \left( \frac{x}{y} \right) \right] - 1.17 \left\{ \sin \left[ 1.31 \ln \left( \frac{x}{y} \right) \right] \right\} \right) \right]. \quad (46) \end{aligned}$$

For my numerical investigation, the high-order corrections to  $F_L(x, Q^2)$  are shown in Fig. 4 and compared with H1 data [1] for  $Q^2 = 20, 45, 200$  and  $500$  GeV<sup>2</sup>. In this figure the straight and dash lines represent the gluonic longitudinal structure function solutions at NLO and NNLO, respectively. These results are obtained with respect to the Laplace transform technique as described in Appendix D. In this figure, the circles represent the longitudinal structure functions from Ref. [1] as accompanied with total errors. These results are in agreement with  $F_L(x, Q^2)$  predicted from the global fit at LO, NLO, and NNLO in Ref. [12]. However, it is a reflection of the behavior of the deep inelastic structure function and the coefficient functions at low values of  $x$ .

In the next sections, the recombination processes between gluons in a dense system have to be taken into account. Therefore the gluonic longitudinal structure function behavior has to be tamed by screening effects.

#### IV. NONLINEAR BEHAVIOR

The screening effects are provided by a multiple gluon interaction which leads to the nonlinear terms in the derivation of the linear DGLAP evolution equations. Therefore, the standard linear DGLAP evolution equations will have to be modified to take the nonlinear corrections into account.

Gribov, Levin, Ryskin, Mueller, and Qiu (GLR-MQ) [14] performed a detailed study of these recombination processes. This widely known as the GLR-MQ equation and involves

the two-gluon distribution per unit area of the hadron. This equation predicts a saturation behavior of the gluon distribution at very small  $x$  [15,16]. A closer examination of the small- $x$  scattering is resummation powers of  $\alpha_s \ln(1/x)$ , which leads to the  $k_T$ -factorization form [17]. In the  $k_T$ -factorization approach, the large logarithms  $\ln(1/x)$  are relevant for the unintegrated gluon density in a nonlinear equation. The solution of this equation develops a saturation scale where tame the gluon density behavior at low values of  $x$ , and this is an intrinsic characteristic of a dense gluon system.

Therefore, one should consider the low- $x$  behavior of the singlet distribution by using the nonlinear GLR-MQ evolution equation. The shadowing correction to the evolution of the singlet quark distribution can be written as [13,14,18]

$$\frac{\partial xq(x, Q^2)}{\partial \ln Q^2} = \frac{\partial xq(x, Q^2)}{\partial \ln Q^2} \Big|_{\text{DGLAP}} - \frac{27\alpha_s^2}{160R^2 Q^2} [xg(x, Q^2)]^2. \quad (47)$$

Equation (47) can be rewritten in a convenient form as

$$\begin{aligned} &\frac{\partial F_2(x, Q^2)}{\partial \ln Q^2} \\ &= \frac{\partial F_2(x, Q^2)}{\partial \ln Q^2} \Big|_{\text{DGLAP}} - \frac{5}{18} \frac{27\alpha_s^2}{160R^2 Q^2} [xg(x, Q^2)]^2. \quad (48) \end{aligned}$$

The first term is the standard DGLAP evolution equation [Eq. (11)] and the value of  $R$  is the correlation radius between

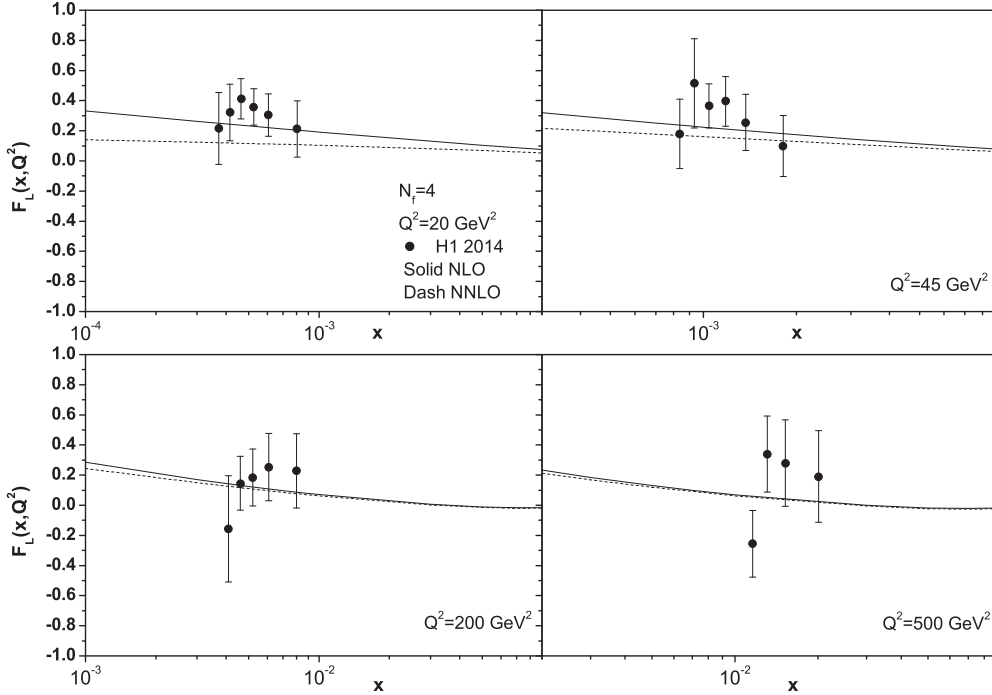


FIG. 4. The high-order corrections to the gluonic longitudinal structure function compared with H1 data [1].

two interacting gluons. It will be of the order of the proton radius ( $R \simeq 5 \text{ GeV}^{-1}$ ), if the gluons are distributed through the whole of proton, or much smaller ( $R \simeq 2 \text{ GeV}^{-1}$ ) if gluons are concentrated in the hot-spot within the proton.

One would find Eq. (48) at LO analysis in  $s$  space as

$$\begin{aligned} \frac{\partial F_2(s, Q^2)}{\partial \ln Q^2} &= \frac{10\alpha_s}{18\pi} G(s, Q^2) \Theta_2^{\text{LO}}(s) \\ &\quad - \frac{5}{18} \frac{27\alpha_s^2}{160R^2 Q^2} G^2(s, Q^2). \end{aligned} \quad (49)$$

The longitudinal structure function in  $s$ -space is given in the following form

$$F_L(s, Q^2) = \frac{20\alpha_s}{9\pi} G(s, Q^2) \Theta_L^{\text{LO}}(s). \quad (50)$$

Combining Eqs. (49) and (50), one could calculate the nonlinear relation between the derivative of the structure function and longitudinal structure function in  $s$  space as I have:

$$\frac{\partial F_2(s, Q^2)}{\partial \ln Q^2} = \frac{h(s)}{4} F_L(s, Q^2) - \frac{\zeta}{\Theta_L^2(s)} F_L^2(s, Q^2), \quad (51)$$

where  $\zeta = \frac{243\pi^2}{25600R^2 Q^2}$ . At  $\zeta \rightarrow 0$ , Eq. (51) leads to the linear relation between the structure functions [i.e., Eq. (21)].

Equation (51) yields the gluonic longitudinal structure function with nonlinear effects as

$$F_L^2(s, Q^2) - \frac{h(s)}{4} \frac{\Theta_L^2(s)}{\zeta} F_L(s, Q^2) + \frac{\Theta_L^2(s)}{\zeta} D F_2(s, Q^2) = 0. \quad (52)$$

It is tempting, however, to discard one of the roots of Eq. (52). The solution of Eq. (52) then leads to a solution for the nonlin-

ear gluonic longitudinal structure function. This equation can be solved by a Taylor series expansion around a particular choice of point of expansion. Since  $(\zeta R^2 Q^2)^n < 1$ , so this series is convergent when  $n \rightarrow \infty$ . This parameter decreases with increasing  $n$ , as seen from Table II. For the longitudinal structure function in  $s$  space, one has

$$\begin{aligned} F_L(s, Q^2) &= 4h^{-1}(s) D F_2(s, Q^2) + 64\zeta \frac{\Theta_L(s)}{\Theta_3^3(s)} D F_2^2(s, Q^2) \\ &\quad + 2048\zeta^2 \frac{\Theta_L(s)}{\Theta_2^5(s)} D F_2^3(s, Q^2) \dots \end{aligned} \quad (53)$$

Equation (53) covers the whole range of expanding, as shown in Table II. The contribution from the fourth term to the second term (such that  $\frac{\text{Fourth term}}{\text{Second term}} \propto \frac{\zeta^3}{\zeta} = \zeta^2$ ) is around the order  $O(\sim 10^{-2})$ . To make a rough estimate of the accuracy in the expansion method I find the longitudinal structure function until a fourth-order approximation with respect to the  $\zeta$  expansion and neglecting the high-order terms  $O(\zeta^3)$  in Eq. (53). For this evolution, I retain the second-order term in  $\zeta$ . Therefore, the gluonic longitudinal structure function in

TABLE II. Higher-order terms in expansion method.

n	$(\zeta R^2 Q^2)^n$
1	$O(10^{-1})$
2	$O(10^{-2})$
3	$O(10^{-3})$
4	$O(10^{-4})$

$\nu$  space is defined as

$$\widehat{F}_L(\nu, Q^2) = 4 \int_0^1 \widehat{DF}_2(\nu, Q^2) \widehat{J}(\nu - \omega) d\omega \quad (54)$$

$$+ \int_0^1 \widehat{DF}_2^2(\nu, Q^2) \widehat{P}(\nu - \omega) d\omega$$

$$+ \int_0^1 \widehat{DF}_2^3(\nu, Q^2) \widehat{T}(\nu - \omega) d\omega, \quad (55)$$

where

$$\widehat{J}(\nu) \equiv \mathcal{L}^{-1}[h^{-1}(s); \nu] \equiv \frac{1}{4} W_1^{\text{LO}}(\nu),$$

$$\widehat{P}(\nu) \equiv \mathcal{L}^{-1}\left[64\zeta \frac{\Theta_L(s)}{\Theta_2^3(s)}; \nu\right] \equiv W_2^{\text{LO}}(\nu, Q^2),$$

$$\widehat{T}(\nu) \equiv \mathcal{L}^{-1}\left[2048\zeta^2 \frac{\Theta_L(s)}{\Theta_2^5(s)}; \nu\right] \equiv W_3^{\text{LO}}(\nu, Q^2).$$

The inverse Laplace transform of kernels can be found in Appendix E. Applying the properties of the Dirac  $\delta$  function, I finally have the nonlinear gluonic longitudinal structure function in  $x$  space in the following form:

$$F_L(x, Q^2)|_{N_f=4}$$

$$= \text{Eq. (26)} + \int_x^1 \widehat{DF}_2^2(\nu, Q^2) W_2^{\text{LO}}(\nu - \omega, Q^2) d\omega$$

$$+ \int_0^1 \widehat{DF}_2^3(\nu, Q^2) W_3^{\text{LO}}(\nu - \omega, Q^2) d\omega, \quad (56)$$

where  $W_1^{\text{LO}}$  is independent of the values of  $Q^2$ , but  $W_2^{\text{LO}}$  and  $W_3^{\text{LO}}$  depend on  $Q^2$ . Thus I obtain an expression for the gluonic longitudinal structure function  $F_L(x, Q^2)$  to leading order by solving the nonlinear GLR-MQ evolution equation. Equation (56) shows that it is independent of the gluon behavior, of the running coupling constant, and also of the QCD cutoff parameter in the LO approximation. One can easily solve this equation [i.e., Eq. (56)] and extract the nonlinear gluonic longitudinal structure function.

The nonlinear behavior of  $F_L(x, Q^2)$  is shown in Fig. 5 for values of  $Q^2 = 6.5$  and  $20 \text{ GeV}^2$ . It would appear that the effect of nonlinearity at low  $x$  should observe for moderate  $Q^2$  when compared with H1 data. In this figure, the nonlinear effect investigated at the hot-spot point ( $R = 2 \text{ GeV}^{-1}$ ). It is shown that the results obtained from the present analysis based on the Laplace transform are in good agreement with those obtained by the H1 Collaboration [1]. The saturation of the gluon density at small  $x$  indirectly is significant for understanding the nonlinear effects in Eq. (56) and also high-order corrections. In the next section I apply high-order corrections to the nonlinear behavior and compared with H1 data.

## V. HIGH-ORDER CORRECTIONS TO THE NONLINEAR BEHAVIOR

Using the formalism given in the previous section, I calculate the high-order corrections to the nonlinear behavior of the gluonic longitudinal structure function in the low- $x$  region. In terms of the derivative of proton structure function with respect

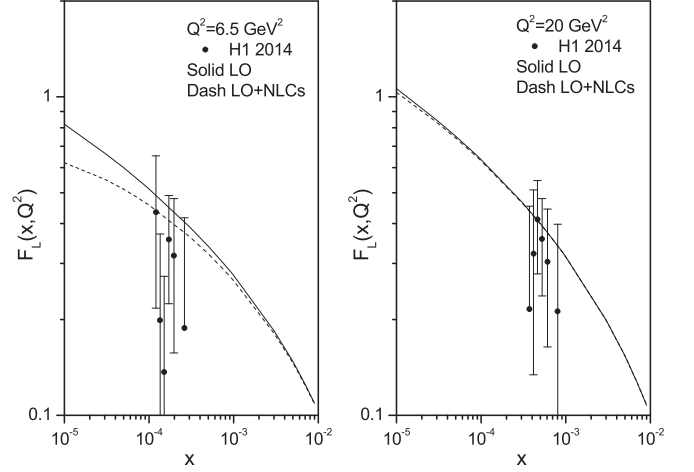


FIG. 5. Nonlinear corrections (NLCs) to the gluonic longitudinal structure function  $F_L$  at LO analysis for  $N_f = 4$  at  $R = 2 \text{ GeV}^{-1}$  compared with H1 data at  $Q^2 = 6.5$  and  $20 \text{ GeV}^2$  (solid points).

to  $\ln Q^2$ , the GLR-MQ evaluation equation can be written with the high-order correction in  $s$  space as

$$\frac{\partial F_2(s, Q^2)}{\partial \ln Q^2} = \frac{5}{18} \frac{\alpha_s(Q^2)}{4\pi} \Theta_2(s, Q^2) g(s, Q^2)$$

$$- \frac{5}{18} \frac{27\alpha_s^2(Q^2)}{160R^2 Q^2} g^2(s, Q^2), \quad (57)$$

where

$\Theta_2(s, Q^2) = \Theta_2^{\text{LO}}(s) + \frac{\alpha_s(Q^2)}{4\pi} \Theta_2^{\text{NLO}}(s) + \left(\frac{\alpha_s(Q^2)}{4\pi}\right)^2 \Theta_2^{\text{NNLO}}(s)$ . One should consider the same method introduced in the previous section: I find the high-order corrections to the gluonic longitudinal structure function in the following form:

$$\frac{\partial F_2(s, Q^2)}{\partial \ln Q^2} = \frac{5}{18} \frac{\Theta_2(s, Q^2)}{\langle e^2 \rangle \Theta_L(s, Q^2)} F_L(s, Q^2)$$

$$- \frac{3\pi^2}{4R^2 Q^2} \frac{F_L^2(s, Q^2)}{[\langle e^2 \rangle \Theta_L(s, Q^2)]^2}, \quad (58)$$

where

$\Theta_L(s, Q^2) = \Theta_L^{\text{LO}}(s) + \frac{\alpha_s(Q^2)}{4\pi} \Theta_L^{\text{NLO}}(s) + \left(\frac{\alpha_s(Q^2)}{4\pi}\right)^2 \Theta_L^{\text{NNLO}}(s)$ . Equation (58) can be solved simultaneously to get the desired nonlinear equation for longitudinal structure function. Using the inverse Laplace transform to go back from  $s$  space to  $x$  space, the simplified solution of the above equation with high-order corrections can be obtained by

$$F_L(x, Q^2) = \text{Eq. (45)} + \mathcal{L}^{-1}\left[\frac{B(s, Q^2)}{A^3(s, Q^2)} D^2 F_2(s, Q^2); \nu\right]$$

$$+ \mathcal{L}^{-1}\left[2 \frac{B^2(s, Q^2)}{A^5(s, Q^2)} D^3 F_2(s, Q^2); \nu\right], \quad (59)$$

where  $A(s, Q^2) = \frac{5}{18} \frac{\Theta_2(s, Q^2)}{\langle e^2 \rangle \Theta_L(s, Q^2)}$  and  $B(s, Q^2) = \frac{3\pi^2}{4R^2 Q^2 [\langle e^2 \rangle \Theta_L(s, Q^2)]^2}$ .

Therefore the solution of the nonlinear corrections at NLO up to NNLO analysis leads us to nonlinear behavior of the gluonic longitudinal structure function at moderate values of

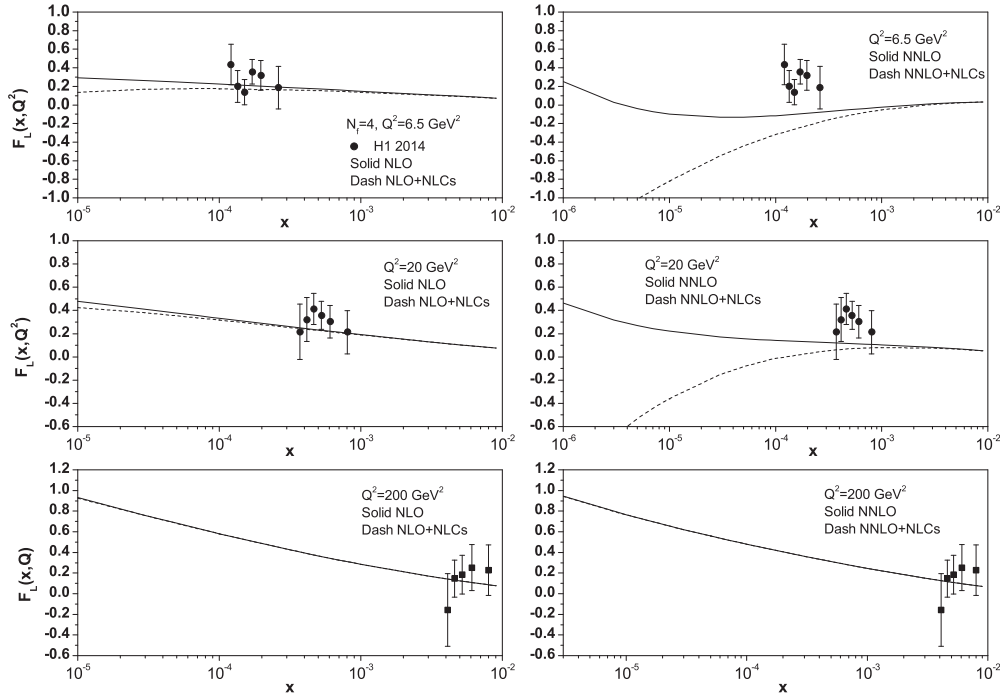


FIG. 6. High-order nonlinear corrections to the gluonic longitudinal structure function  $F_L$  at NLO up to NNLO analysis for  $N_f = 4$  at  $R = 2 \text{ GeV}^{-1}$  compared with H1 data at  $Q^2 = 6.5, 20, \text{ and } 200 \text{ GeV}^2$  (solid points).

$Q^2$ . The analytical expressions for these corrections are given in Appendix F. The validity of the nonlinear corrections to the DGLAP evolution equation is in the region of small  $x$  and intermediate values of  $Q^2$ . The nonlinear corrections can be neglected at large values of  $Q^2$ , so I expect that my result is valid in the kinematic region  $x \leq 0.01$  and moderate  $Q^2$ .

In Fig. 6 the nonlinear behavior for moderate and high  $Q^2$  values are shown. One would expect this behavior to be observed at moderate  $Q^2$  values, as considered in Fig. 6. From these figures, it is observed that the NLO nonlinear corrections (NLO + NLCs) show tamed behavior compared with those obtained from only NLO corrections when compared with H1 data. It is observed that NNLO nonlinear corrections (NNLO + NLCs) have a negative rate as  $x$  decreases at moderate  $Q^2$  values.

Indeed, comparison of the NNLO + NLCs with the NNLO calculations shows a turnover of the gluonic longitudinal structure function at  $Q^2 = 6.5$  and  $20 \text{ GeV}^2$ . This is due to the effect of the gluonic coefficient function to the gluonic splitting function ratio, which decreases the limit NNLO corrections when tamed with respect to the nonlinear saturation effect. Since gluon recombination introduces a negative correction to the NNLO linear behavior, the signal of its presence is a decrease of the scaling violation and this is strongly dependent on the correlation radius (i.e.,  $R$ ). In Fig. 7, the effect of the nonlinearity in NNLO results for  $R = 4 \text{ GeV}^{-1}$  at  $Q^2 = 6.5$  and  $20 \text{ GeV}^2$  investigated. It can be observed (in Figs. 6 and 7) that NNLO results are very sensitive to  $R$  as  $x$  decreases. Indeed the effect of third-order corrections to the coefficients functions and splitting functions at hot-spot points decrease the gluonic longitudinal structure function to the negative values as  $x$  decreases. This behavior is comparable when  $R$  increase throughout the entire proton at NNLO approximation.

At least there is another mechanism to prevent generation of the high-density gluon states; namely, the well-known vacuum color screening [19]. There is a transition between the nonperturbative and perturbative domains. In the QCD vacuum, the nonperturbative fields form structures with sizes  $\sim R_c$  which it is smaller than  $\Lambda_{\text{QCD}}$ . The short propagation length for perturbative gluons is  $R_c \sim 0.2\text{--}0.3 \text{ fm}$ .

The gluon fusion effect in nonlinear regime controlled by the new dimensionless parameter  $\sim \frac{R_c^2}{8B}$  where  $B$  is the characteristic size of the interaction region because this parameter can be defined by  $\ln(x_0/x)$  and  $r$  where  $r^2 \sim Q^{-2}$ . In all figures one should observe that the nonlinear effects are small even

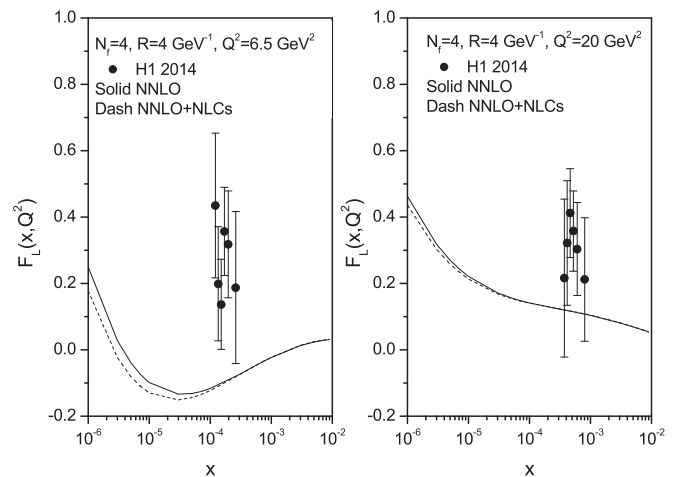


FIG. 7. NNLO nonlinear corrections to the gluonic longitudinal structure function  $F_L$  for  $N_f = 4$  at  $R = 4 \text{ GeV}^{-1}$  compared with H1 data at  $Q^2 = 6.5$  and  $20 \text{ GeV}^2$  (solid points).

at lowest  $x$  values. This behavior is in accordance with the smallness of the ratio  $\frac{K_c^2}{8B}$ . It is interesting to look at the nonlinear limit where decreases as  $Q^2$  increases. From [19], the nonlinear effects leads to the logarithmically ratio as the nonlinear/linear effects are proportional to  $R_c^2/8B(\ln(x_0/x), r^2) \ln(Q^2 R_c^2)$ . Figure 6 shows that high-order corrections to the nonlinear behavior are very small at high  $Q^2$  values and at the lowest available Bjorken  $x$ .

## VI. CONCLUSION

In this paper I have estimated an analytical solution for the linear and nonlinear behavior of the longitudinal structure function with respect to the derivative of the proton structure function inside the proton.

This solution is independent of the gluon model and the running coupling constant at leading-order analysis and it is free of any point expanding model for the gluon distribution behavior. The ratio of splitting functions applying the Laplace transform technique are calculated. I have used the heavy coefficient functions for heavy-flavor production in DIS in the fixed-flavor-number scheme (FFNS) with  $N_f = 3$ . In the present calculations the high-order corrections (NLO and NNLO) for structure functions at low  $x$  values, arising from the coefficient functions and the splitting functions, are obtained. I have therefore used from these results for the gluonic longitudinal structure function at moderate and high values of  $Q^2$ .

The nonlinear GLR-MQ evolution equation predicted by considering the general Laplace transform method and studied

the effects of adding the nonlinear corrections to the linear longitudinal structure function at the hot-spot point ( $R = 2 \text{ GeV}^{-1}$ ) with  $N_f = 4$ . For the gluonic longitudinal structure function the nonlinear effects are found to play an increasingly important role at  $x \leq 10^{-3}$ . I have incorporated high-order corrections to the nonlinear behavior in the kinematic range of moderate  $Q^2$  and obtained the nonlinear longitudinal structure function at low  $x$  at the NLO and NNLO approximations. It is interesting to see that the NNLO analysis at moderate  $Q^2$  depends on the proton radius as the nonlinear behavior increases as  $R$  increases. This is due to the contribution from the NNLO terms in the ratio of coefficient function to the splitting function. It can be observed that, with decreasing  $x$ , the taming of  $F_L(x, Q^2)$  is apparently observed in the NLO approximation at  $R = 2 \text{ GeV}^{-1}$  and in the NNLO approximation at  $R = 4 \text{ GeV}^{-1}$ . The method presented in this analysis enables us to achieve strictly analytical linear and nonlinear solutions at LO to NNLO approximation for the gluonic longitudinal structure function in terms of the derivative of the proton structure function with respect to  $\ln Q^2$  at low values of  $x$ . The nonlinear effects are shown to be small at large  $Q^2$ , even at lowest Bjorken values of  $x$ .

## ACKNOWLEDGMENTS

Author thanks Urs A. Wiedemann for discussions which completed this study and the Department of Physics of the CERN-TH for their warm hospitality. Also I would like to thank M. Tabrizi for his careful editorial revising of the paper.

## APPENDIX A

The kernels at leading order analysis are as follows:

$$P_{qg}^{\text{LO}}(z) = z^2 + (1-z)^2, \quad (\text{A1})$$

and

$$c_{L,g}^{\text{LO}}(z) = z^2(1-z). \quad (\text{A2})$$

The parameters  $\hat{J}^c(v)$  and  $\hat{J}^b(v)$  are given in the following form: At  $Q^2 = 20 \text{ GeV}^2$ ,

$$\begin{aligned} \hat{J}^c(v) &= 0.252 \exp(-3.183v) \cos(0.198v) + 0.424 \exp(-3.183v) \sin(0.198v) - 0.0232 \exp(-2.050v) \\ &\quad - 0.0624 \exp(-1.127v) \cos(0.305v) - 0.0692 \exp(-1.127v) \sin(0.305v) + 0.156\delta(v), \\ \hat{J}^b(v) &= -4.035 \exp(-7.471v) - 0.0745 \exp(-2.246v) + 0.0445 \exp(-1.313v) \cos(0.393v) \\ &\quad - 0.154 \exp(-1.313v) \sin(0.393v) + 0.370 \exp(-0.310v) + 1.405\delta(v). \end{aligned} \quad (\text{A3})$$

At  $Q^2 = 200 \text{ GeV}^2$ ,

$$\begin{aligned} \hat{J}^c(v) &= -0.0164 \exp(-3.169v) + 0.111 \exp(-2.609v) - 0.003 \exp(-2.005v) \\ &\quad - 0.0912 \exp(-1.164v) \cos(0.218v) - 0.0293 \exp(-1.164v) \sin(0.218v) + 0.228\delta(v), \\ \hat{J}^b(v) &= 0.222 \exp(-3.146v) \cos(0.152v) + 0.518 \exp(-3.146v) \sin(0.152v) - 0.0212 \exp(-2.046v) \\ &\quad - 0.0645 \exp(-1.127v) \cos(0.299v) - 0.0685 \exp(-1.127v) \sin(0.299v) + 0.171\delta(v). \end{aligned} \quad (\text{A4})$$

## APPENDIX B

The proton structure function parametrized with a global fit function [9] to the HERA combined data for  $F_2^{\gamma p}(x, Q^2)$  for  $0.85 < Q^2 < 3000 \text{ GeV}^2$  and  $x < 0.1$ , which ensures that the saturated Froissart  $\ln^2(1/x)$  behavior dominates at small  $x$ . This

global fit takes the form

$$F_2^{\gamma p}(x, Q^2) = (1-x) \left[ \frac{F_P}{1-x_P} + A(Q^2) \ln \left( \frac{x_P}{x} \frac{1-x}{1-x_P} \right) B(Q^2) \ln^2 \left( \frac{x_P}{x} \frac{1-x}{1-x_P} \right) \right], \quad (\text{B1})$$

where

$$A(Q^2) = a_0 + a_1 \ln Q^2 + a_2 \ln^2 Q^2,$$

and

$$B(Q^2) = b_0 + b_1 \ln Q^2 + b_2 \ln^2 Q^2.$$

The fitted parameters are tabulated in Table I. At small  $x$  [or large  $\nu = \ln(1/x)$ ], the global fit becomes a quadratic polynomial in  $\nu$  because  $\widehat{F}_2^{\gamma p}(\nu, Q^2) \rightarrow C_{0f}(Q^2) + C_{1f}(Q^2)\nu + C_{2f}(Q^2)\nu^2 + \widehat{O}(\nu)$  where the coefficient functions are defined in Ref. [9].

### APPENDIX C

At small  $x$  the one-loop up to three-loop splitting functions for  $N_f = 4$  read

$$\begin{aligned} P^{\text{LO}} &= 2N_f(1-2x+2x^2), \\ P^{\text{NLO}} &\rightarrow C_A T_f \frac{40}{9x}, \\ P^{\text{NNLO}} &\rightarrow E_1^{qg} \frac{\ln x}{x} + E_2^{qg} \frac{1}{x}, \end{aligned} \quad (\text{C1})$$

where  $E_1^{qg} \simeq -298.667N_f$  and  $E_2^{qg} \simeq -1268.28N_f + 4.57613N_f^2$ . The gluonic longitudinal coefficient functions up to NNLO analysis at small  $x$  can be written as

$$\begin{aligned} c^{\text{LO}} &= 8N_f x(1-x), \\ c^{\text{NLO}} &\rightarrow \frac{-5.333N_f}{x} + (-6.229N_f + 0.8889N_f^2), \\ c^{\text{NNLO}} &\rightarrow N_f \left( \frac{-2044.70}{x} - 409.506 \frac{\ln x}{x} \right) + N_f^2 \frac{88.5037}{x}. \end{aligned} \quad (\text{C2})$$

### APPENDIX D

The high-order ratios for some of  $Q^2$  values at NLO and NNLO analysis are

$$\begin{aligned} H^{\text{NLO}}(\nu, 20) &= \exp(-1.54\nu)[3.73 \cos(1.33\nu) - 1.68 \sin(1.33\nu)] - 0.13 \exp(-0.82E - 1\nu) - 0.68E - 1\delta(\nu), \\ H^{\text{NNLO}}(\nu, 20) &= \exp(-1.40\nu)[3.82 \cos(1.31\nu) - 1.17 \sin(1.31\nu)] + \exp(+0.59\nu)[-0.30 \cos(0.26\nu) + 0.11 \sin(0.26\nu)] \\ &\quad - 0.31\delta(\nu), \\ H^{\text{NLO}}(\nu, 45) &= \exp(-1.54\nu)[3.77 \cos(1.33\nu) - 1.66 \sin(1.33\nu)] - 0.12 \exp(-0.73E - 1\nu) - 0.60E - 1\delta(\nu), \\ H^{\text{NNLO}}(\nu, 45) &= \exp(-1.43\nu)[3.84 \cos(1.32\nu) - 1.25 \sin(1.32\nu)] + \exp(+0.04\nu)[-0.24 \cos(0.23\nu) + 0.01 \sin(0.23\nu)] \\ &\quad - 0.25\delta(\nu), \\ H^{\text{NLO}}(\nu, 200) &= \exp(-1.53\nu)[3.81 \cos(1.33\nu) - 1.64 \sin(1.33\nu)] - 0.10 \exp(-0.61E - 1\nu) - 0.50E - 1\delta(\nu), \\ H^{\text{NNLO}}(\nu, 200) &= \exp(-1.45\nu)[3.87 \cos(1.32\nu) - 1.35 \sin(1.32\nu)] + \exp(+0.22E - 1\nu)[-0.17 \cos(0.19\nu) \\ &\quad + 0.85 \sin(0.19\nu)] - 0.18\delta(\nu), \\ H^{\text{NLO}}(\nu, 500) &= \exp(-1.53\nu)[3.83 \cos(1.33\nu) - 1.63 \sin(1.33\nu)] - 0.91E - 1 \exp(-0.55E - 1\nu) - 0.45E - 1\delta(\nu), \\ H^{\text{NNLO}}(\nu, 500) &= \exp(-1.46\nu)[3.88 \cos(1.32\nu) - 1.39 \sin(1.32\nu)] + \exp(+0.16E - 1\nu)[-0.15 \cos(0.17\nu) \\ &\quad + 0.78E - 1 \sin(0.17\nu)] - 0.15\delta(\nu). \end{aligned} \quad (\text{D1})$$

## APPENDIX E

The inverse-Laplace of the nonlinear kernels is as follows:

$$\widehat{J}(v) = \text{Eq. (26)},$$

$$\begin{aligned} \widehat{P}(v) = & \zeta[(-56768/343\sqrt{7} + 3328/49\sqrt{7}v + 1408/49v^2\sqrt{7}) \sin(1/2\sqrt{7}v) \exp(-3/2v) \\ & + (-20224/49v + 128/7v^2 - 320) \exp(-3/2v) \cos(1/2\sqrt{7}v) + 64\delta'(v) + 256\delta(v)], \end{aligned}$$

$$\begin{aligned} \widehat{T}(v) = & \zeta^2[(145\,276\,928/2401\sqrt{7}v - 40\,165\,376/2401v^2\sqrt{7} + 203\,331\,584/2401\sqrt{7} - 3\,866\,624/1029v^3\sqrt{7} \\ & + 20\,480/1029v^4\sqrt{7}) \sin(1/2\sqrt{7}v) \exp(-3/2v) + (-3\,604\,480/1029v^3 + 63\,062\,016/343v \\ & + 22\,896\,640/343v^2 - 69\,632/147v^4 - 100\,352) \exp(-3/2v) \cos(1/2\sqrt{7}v) + 2048\delta(3,v) + 20\,480\delta(2,v) \\ & + 49\,152\delta(1,v) - 61\,440\delta(v)], \end{aligned}$$

$$W_1^{\text{LO}}(v,6.5) = -0.57 \exp(-1.5v)[-7 \cos(1.32v) + 2.64 \sin(1.32v)],$$

$$\begin{aligned} W_2^{\text{LO}}(v,6.5) = & 0.92\delta(v) + 0.23\delta(1,v) + \exp(-1.5v)[(-1.153 - 1.49v + 0.066v^2) \cos(1.32v) \\ & + (-1.58 + 0.65v + 0.27v^2) \sin(1.32v)], \end{aligned}$$

$$\begin{aligned} W_3^{\text{LO}}(v,6.5) = & -0.8\delta(v) + 0.64\delta(1,v) + 0.27\delta(2,v) + 0.026\delta(3,v) \\ & + \exp(-1.5v)[(-1.3 + 2.39v + 0.87v^2 - 0.045v^3 - 0.006v^4) \cos(1.32v) \\ & + (2.91 + 2.08v - 0.57v^2 - 0.13v^3 + 0.0007v^4) \sin(1.32v)], \end{aligned}$$

$$W_1^{\text{LO}}(v,20) = \text{Constant}(W_1^{\text{LO}}(v,6.5)),$$

$$\begin{aligned} W_2^{\text{LO}}(v,20) = & 0.30\delta(v) + 0.075\delta(1,v) + \exp(-1.5v)[(-0.37 - 0.48v + 0.02v^2) \cos(1.32v) \\ & + (-0.51 + 0.21v + 0.09v^2) \sin(1.32v)], \end{aligned}$$

$$\begin{aligned} W_3^{\text{LO}}(v,20) = & -0.084\delta(v) + 0.067\delta(1,v) + 0.03\delta(2,v) + 0.003\delta(3,v) + \exp(-1.5v)[(-0.14 + 0.25v + 0.09v^2 - 0.005v^3 \\ & - 0.0006v^4) \cos(1.32v) + (0.31 + 0.22v - 0.061v^2 - 0.014v^3 + 0.000\,07v^4) \sin(1.32v)]. \end{aligned} \quad (\text{E1})$$

## APPENDIX F

The nonlinear corrections for some of  $Q^2$  values at NLO up to NNLO analysis are

$$W_1^{\text{NLO}}(v,6.5) = -0.08\delta(v) - 0.15 \exp(-0.1v) + \exp(-1.55v)[3.67 \cos(1.33v) - 1.70 \sin(1.33v)],$$

$$\begin{aligned} W_2^{\text{NLO}}(v,6.5) = & 0.57\delta(v) + 0.15\delta(1,v) - 0.004\delta(2,v) + \exp(-1.55v)[(-1.17 - 1.02v + 0.13v^2) \cos(1.33v) \\ & + (-0.99 + 0.86v + 0.2v^2) \sin(1.33v)] + \exp(-0.1v)(-0.016 + 0.003v - 0.000\,06v^2), \end{aligned}$$

$$\begin{aligned} W_3^{\text{NLO}}(v,6.5) = & -0.74\delta(v) + 0.25\delta(1,v) + 0.14\delta(2,v) + 0.013\delta(3,v) - 0.0004\delta(4,v) \\ & + \exp(-1.55v)[(-0.017 + 2.15v + 0.35v^2 - 0.08v^3 - 0.004v^4) \cos(1.33v) \\ & + (2.15 + 0.55v - 0.67v^2 - 0.06v^3 + 0.003v^4) \sin(1.33v)] \\ & + \exp(-0.1v)(-0.0002 + 0.0006v - 0.000\,06v^2 + 0.13E - 5v^3 - 0.84E - 8v^4), \end{aligned}$$

$$\begin{aligned} W_1^{\text{NNLO}}(v,6.5) = & -0.45\delta(v) + \exp(0.1v)[-0.50 \cos(0.31v) + 0.10 \sin(0.31v)] + \exp(-1.35v)[3.76 \cos(1.3v) \\ & - 0.99 \sin(1.3v)], \end{aligned}$$

$$\begin{aligned} W_2^{\text{NNLO}}(v,6.5) = & 0.98\delta(v) + 0.014\delta(1,v) - 0.036\delta(2,v) + \exp(-1.35v)[(0.12 - 1.85v - 0.18v^2) \cos(1.3v) \\ & + (-2.38 - 0.65v + 0.28v^2) \sin(1.3v)] + \exp(0.1v)[(-0.18 - 0.014v + 0.002v^2) \cos(0.31v) \\ & + (-0.045 + 0.04v + 0.001v^2) \sin(0.31v)], \end{aligned}$$

$$\begin{aligned} W_3^{\text{NNLO}}(v,6.5) = & 0.76\delta(v) + 1.2\delta(1,v) + 0.11\delta(2,v) - 0.04\delta(3,v) - 0.006\delta(4,v) \\ & + \exp(-1.35v)[(-5.69 - 2.3v + 1.22v^2 + 0.2v^3 - 0.001v^4) \cos(1.3v) \\ & + (-0.22 + 5v + 1.23v^2 - 0.1v^3 - 0.01v^4) \sin(1.3v)] \\ & + \exp(0.1v)[(-0.26 - 0.011v + 0.007v^2 + 0.0002v^3 - 0.12E - 5v^4) \cos(0.31v) \\ & + (0.047 + 0.08v + 0.004v^2 - 0.0002v^3 - 0.35E - 5v^4) \sin(0.31v)], \end{aligned} \quad (\text{F1})$$

and

$$\begin{aligned}
W_1^{\text{NLO}}(\nu, 20) &= -0.07\delta(\nu) - 0.13 \exp(-0.082\nu) + \exp(-1.54\nu)[3.73 \cos(1.33\nu) - 1.68 \sin(1.33\nu)], \\
W_2^{\text{NLO}}(\nu, 20) &= 0.20\delta(\nu) + 0.054\delta(1, \nu) - 0.001\delta(2, \nu) + \exp(-1.54\nu)[(-0.38 - 0.36\nu + 0.04\nu^2) \cos(1.33\nu) \\
&\quad + (-0.35 + 0.27\nu + 0.07\nu^2) \sin(1.33\nu)] + \exp(-0.082\nu)(-0.005 + 0.0007\nu - 0.00001\nu^2), \\
W_3^{\text{NLO}}(\nu, 20) &= -0.082\delta(\nu) + 0.032\delta(1, \nu) + 0.02\delta(2, \nu) + 0.002\delta(3, \nu) - 0.00004\delta(4, \nu) \\
&\quad + \exp(-1.54\nu)[(-0.02 + 0.24\nu + 0.05\nu^2 - 0.008\nu^3 - 0.0004\nu^4) \cos(1.33\nu) \\
&\quad + (+0.24 + 0.083\nu - 0.07\nu^2 - 0.008\nu^3 + 0.0003\nu^4) \sin(1.33\nu)] \\
&\quad + \exp(-0.082\nu)(-0.0001 + 0.00007\nu - 0.45E - 5\nu^2 + 0.8E - 7\nu^3 - 0.4E - 9\nu^4), \\
W_1^{\text{NNLO}}(\nu, 20) &= -0.31\delta(\nu) + \exp(0.06\nu)[-0.30 \cos(0.26\nu) + 0.11 \sin(0.26\nu)] + \exp(-1.4\nu)[3.82 \cos(1.31\nu) \\
&\quad - 1.17 \sin(1.31\nu)], \\
W_2^{\text{NNLO}}(\nu, 20) &= 0.32\delta(\nu) + 0.034\delta(1, \nu) - 0.007\delta(2, \nu) + \exp(-1.4\nu)((-0.15 - 0.6\nu - 0.028\nu^2) \cos(1.31\nu) \\
&\quad + (-0.71 - 0.035\nu + 0.1\nu^2) \sin(1.31\nu)) + \exp(0.06\nu)[(-0.26 - 0.0006\nu + 0.0002\nu^2) \cos(0.26\nu) \\
&\quad + (-0.01 + 0.005\nu + 0.00001\nu^2) \sin(0.26\nu)], \\
W_3^{\text{NNLO}}(\nu, 20) &= -0.011\delta(\nu) + 0.11\delta(1, \nu) + 0.023\delta(2, \nu) - 0.0007\delta(3, \nu) - 0.0003\delta(4, \nu) \\
&\quad + \exp(-1.4\nu)[(-0.45 + 0.025\nu + 0.15\nu^2 + 0.11\nu^3 - 0.0006\nu^4) \cos(1.31\nu) \\
&\quad + (0.20 + 0.48\nu + 0.042\nu^2 - 0.017\nu^3 - 0.0007\nu^4) \sin(1.31\nu)], \\
&\quad + \exp(0.06\nu)[(-0.008 - 0.00004\nu + 0.0001\nu^2 + 0.13E - 4\nu^3 - 0.44E - 7\nu^4) \cos(0.26\nu) \\
&\quad + (0.001 + 0.002\nu + 0.00002\nu^2 - 0.45E - 5\nu^3 - 0.23E - 7\nu^4) \sin(0.26\nu)], \tag{F2}
\end{aligned}$$

where  $W_s$  are inverse Laplace transforms of all coefficients at LO up to NNLO analysis in accordance with the results expanded in nonlinear behavior.

- 
- [1] V. Andreev *et al.* (H1 Collaboration), *Eur. Phys. J. C* **74**, 2814 (2014).  
[2] H. Abramowicz *et al.* (H1 and ZEUS Collaborations), *Eur. Phys. J. C* **75**, 580 (2015).  
[3] A. M. Cooper-Sarkar *et al.*, *Z. Phys. C: Part. Fields* **39**, 281 (1988).  
[4] K. Prytz, *Phys. Lett. B* **311**, 286 (1993).  
[5] M. B. Gay Ducati and P. B. Goncalves, *Phys. Lett. B* **390**, 401 (1997).  
[6] G. R. Boroun and B. Rezaei, *Eur. Phys. J. C* **72**, 2221 (2012).  
[7] M. M. Block, L. Durand, and D. W. McKay, *Phys. Rev. D* **79**, 014031 (2009).  
[8] O. Zenaiev, *Eur. Phys. J. C* **77**, 151 (2017); A. V. Kotikov, *J. Exp. Theor. Phys.* **80**, 979 (1995); A. V. Kotikov and G. Parente, *Mod. Phys. Lett. A* **12**, 963 (1997); *J. Exp. Theor. Phys.* **85**, 17 (1997).  
[9] M. M. Block, L. Durand, P. Ha, and D. W. McKay, *Phys. Rev. D* **88**, 014006 (2013).  
[10] N. N. Nikolaev and V. R. Zoller, *Phys. Lett. B* **509**, 283 (2001); *Phys. At. Nucl.* **73**, 672 (2010); M. Glück, C. Pisano, and E. Reya, *Phys. Rev. D* **77**, 074002 (2008).  
[11] M. M. Block *et al.*, *Eur. Phys. J. C* **69**, 425 (2010); H. Khanpour, A. Mirjalili, and S. A. Tehrani, *Phys. Rev. C* **95**, 035201 (2017); S. Shoeibi *et al.*, [arXiv:1710.06329](https://arxiv.org/abs/1710.06329).  
[12] S. Moch *et al.*, *Phys. Lett. B* **606**, 123 (2005); A. D. Martin *et al.*, *ibid.* **635**, 305 (2006); **636**, 259 (2006); R. S. Thorne, [arXiv:hep/0511351](https://arxiv.org/abs/hep/0511351).  
[13] A. Vogt *et al.*, *Nucl. Phys. B* **691**, 129 (2004); C. D. White and R. S. Thorne, *Eur. Phys. J. C* **45**, 179 (2006).  
[14] A. H. Mueller and J. Qiu, *Nucl. Phys. B* **268**, 427 (1986); L. V. Gribov, E. M. Levin, and M. G. Ryskin, *Phys. Rep.* **100**, 1 (1983).  
[15] G. R. Boroun and B. Rezaei, *Chin. Phys. Lett.* **32**, 111101 (2015); B. Rezaei and G. R. Boroun, *Phys. Lett. B* **692**, 247 (2010); G. R. Boroun, *Eur. Phys. J. A* **43**, 335 (2010).  
[16] M. Devese and J. K. Sarma, *Nucl. Phys. B* **885**, 571 (2014); *Eur. Phys. J. C* **74**, 2751 (2014).  
[17] N. N. Nikolaev and W. Schäfer, *Phys. Rev. D* **74**, 014023 (2006).  
[18] K. J. Eskola *et al.*, *Nucl. Phys. B* **660**, 211 (2003).  
[19] R. Fiore, P. V. Sasorov, and V. R. Zoller, *JETP Lett.* **96**, 687 (2013); R. Fiore, N. N. Nikolaev, and V. R. Zoller, *ibid.* **99**, 363 (2014).